Room-Temperature Microfluidics Packaging Using Sequential Plasma Activation Process

M. M. R. Howlader, S. Suehara, H. Takagi, T. H. Kim, R. Maeda, and T. Suga

***Abstract*—A sequential plasma activation process consisting of oxygen reactive ion etching (RIE) plasma and nitrogen radical plasma was applied for microfluidics packaging at room temperature. Si/glass and glass/glass wafers were activated by the oxygen RIE plasma followed by nitrogen microwave radicals. Then, the activated wafers were brought into contact in atmospheric pressure air with hand-applied pressure where they remained for 24 h. The wafers were bonded throughout the entire area and the bonding strength of the interface was as strong as the parents bulk wafers without any post-annealing process or wet chemical cleaning steps. Bonding strength considerably increased with the nitrogen radical treatment after oxygen RIE activation prior to bonding. Chemical reliability tests showed that the bonded interfaces of Si/Si could significantly withstand exposure to various microfluidics chemicals. Si/glass and glass/glass cavities formed by the sequential plasma activation process indicated hermetic sealing behavior. SiO_xN_y was observed in the sequentially plasma-treated glass wafer, and it is attributed to binding of nitrogen with Si and oxygen and the implantation of N_2 radical in the wafer. High bonding strength observed is attributed to a diffusion of absorbing water onto the wafer surfaces and a reaction between silicon oxynitride layers on the mating wafers. T-shape microfluidic channels were fabricated on glass wafers by bulk micromachining and the sequential plasma-activated bonding process at room temperature.**

***Index Terms*—Bonding strength, glass, hermetic sealing, microfluidic device, nitrogen radical plasma, oxygen reactive ion etching (RIE) plasma, sequential plasma activation process.**

I. Introduction

GLASS substrates have strong insulating and nonreacting behavior to most standard chemicals and are considered for many chemical and biomedical applications as microfluidics devices. Microparticle detection and counting, identification of microparticle types using fluorescence, and blood cell analysis are a few specific applications for microfluidics devices. A number of papers have appeared on DNA sequencing, particles filtering, biochemical analysis, and semen testing for such applications [1]–[3]. Fabrication process of microfluidics devices has matured more than that of their assembly, bonding, and packaging. The integration of glass microfluidics devices requires bonding between the chip and the substrate. Many of the previous approaches used anodic bonding [4], [5], electrostatic bonding [6], adhesive layer bonding [7], or high-temperature bonding processes [8], [9] for the packaging. However, these bonding processes have several disadvantages. Without intermediate layers, glass/glass cannot be bonded anodically. Alkaline ions segregated across the interface during bonding may disturb the biological and chemical species. Solvent extraction and analyte adsorption of the adhesive may limit the performance of microfluidic devices in the adhesive bonding case. In addition, the adhesive and polymerized bonding processes have a severe optical loss problem compared to the direct bonding process. On the other hand, glass and quartz wafers bonded at 650 °C–1000 °C for the integration may collapse and/or distort the channel especially across the bonding edge. Plasma-activated bonding with energetic neutral Ar atoms and reactive H_2O and NH_3 molecules for chip size Si_2/SiO_2 has been reported in high vacuum [10]. Hydrophilic bonding of Si/SiO_2 after N_2, Ar, and O_2 plasma treatment has found similar results in the atmospheric air and vacuum at 200 °C [11]. Nevertheless, the process complexity of plasma activation followed by chemical cleaning is undesirable to many microelectromechanical systems (MEMS) and microfluidics especially to preserving life cell species. To the best of our knowledge, no room-temperature wafer-level bonding for glass/glass wafers, which is a candidate material for microfluidics device as previously mentioned, has been reported. Moreover, the bonding of the patterned wafers is difficult compared with the bare wafers and, therefore, hermetic sealing will be more challenging.

In order to avoid the bonding issues of microfluidics devices, a room-temperature direct wafer bonding technique called sequential plasma activation process for silicon/glass and glass/glass was developed, which can be applicable to the fabrication of microfluidics devices. Glass/glass wafers were integrated for the first time in the atmospheric air at room temperature by the sequential plasma activation process, in which the mating surfaces were cleaned with O_2 radio frequency (RF) plasma followed by N_2 microwave radicals. The bonding load used was significantly low. The interface had a very strong bonding strength comparable to bulk materials and it maintained hermetic sealing. The sequential plasma activation process is different from other microfluidic packaging approaches because it can create hermetic sealed interface with strong bonding strength at low temperature. Paramount

Manuscript received March 3, 2005; revised June 17, 2005.

M. M. R. Howlader is with the Engineering Physics Department and the Electrical and Computer Engineering Department, McMaster University, Hamilton, ON L8S 4LS, Canada (e-mail: mrhowlader@ece.mcmaster.ca).

T. Suga is with the Research Center for Advanced Science and Technology, University of Tokyo, Tokyo 153-8904, Japan (e-mail: Matiar@su.rcast.u-tokyo.ac.jp).

S. Suehara was with the Research Center for Advanced Science and Technology, University of Tokyo, Tokyo 153-8904, Japan. He is now with the Terumo Corporation, Ltd., Tokyo 151, Japan.

T. H. Kim was with the Research Center for Advanced Science and Technology, University of Tokyo, Tokyo 153-8904, Japan. He is now with LG Electronics, Seoul 150-721, South Korea.

H. Takagi and R. Maeda are with the Microelectronic Packaging Laboratory, National Institute for Advanced Industrial Science and Technology, Ibaraki 305-8564, Japan.

Digital Object Identifier 10.1109/TADVP.2006.875070

1521-3323/$20.00 © 2006 IEEE

influence of N_2 radicals on the adhesion enhancement of Si/Si bonding was observed. Since microfluidic devices are essentially important for chemical analysis/reaction in the MEMS-based chemical reactor, the fundamental understanding of chemical influence on the bonding interface would be beneficial. This paper presents the bonding results on bare glass/bare glass, rectangular cavities on Si/bare glass, and glass with holes/glass with microfluidics channels, and addresses several critical issues such as the influence of N_2 pressure on the bonding strength, hermetic sealing behavior, and bonding mechanism and chemical reliability of the interfaces.

II. Experimental Procedure

A. Activation Process and Sample Preparation

Single side mirror-polished 4-in single crystalline Si (100) and both sides mirror-polished 4-in glass wafers were used in this experiment. The thicknesses of the Si and glass wafers were 450 and 1000 μm, respectively. Rectangular and channel structures were fabricated on the chip-size and wafer-level samples by using the standard bulk micromachining process unless otherwise mentioned. Wafer-level surface activated bonding (SAB) tool consisting of nine chambers [12], which were equipped with argon fast atom beam (Ar-FAB) and low-energy ion beam (processing chamber), and RF and microwave (MW) plasma sources (plasma chamber) were used to activate the chip-size and wafer-level sample surfaces. Wafer surfaces were activated in a low vacuum pressure using 13.85-MHz oxygen RF plasma followed by 2.45-GHz MW plasma at room temperature unless otherwise mentioned. In the case of MW plasma, a system to extract electrically neutral radicals was developed. Radicals can chemically activate the wafer surfaces. On the other hand, ions generated in reactive ion etching (RIE) in the RF plasma were accelerated by self-bias voltage to increase physical bombardment capability. The plasma source powers were 200 and 2000 W, respectively, for the RF and MW plasma.

For sequential activation, the wafer surfaces were processed by oxygen RIE plasma for 60 s and then subsequently processed by additional nitrogen radicals for 60 s at 30 Pa unless otherwise mentioned. In order to generate RIE plasma and radicals in one chamber, an RF discharge electrode and an ion-trapping metal plate for MW plasma were used as shown in Fig. 1. In this configuration, RIE plasma is generated by the discharge between the ion trapping metal plate and the RF electrode [Fig. 1(a)]. MW plasma was generated and passed through the ion-trapping metal plate to generate neutralized nitrogen beam (charge-free radicals) by absorbing ions in the holes of the metal plate [Fig. 1(b)]. By the help of the independent plasma generation with the MW and RF discharge systems, a wafer surface can be activated by the ions with high bombarding energy, and the radicals without bombarding energy in one plasma chamber. Oxygen gas for RIE plasma and nitrogen gas for radical generation were used. The plasma discharge and wafer processing conditions are shown in Table I.

Buffered hydrofluoric (BHF) acid was used for the etching of glass wafers to make various structures and channels. The etching rate of glass was 75 nm/min. The patterned chips/wafers were cleaned with acetone and ethanol to remove resists. The samples were then cleaned with H_2SO_4 and H_2O_2 solution at 80 °C followed by HF dip. The samples were rinsed in water after each chemical treatment. Finally, the samples were spun-dried. Nevertheless, the bare glass wafers were not cleaned with any wet chemicals. As received glass wafers were used for the bonding experiments. After surface activations with the sequential plasma activation process, the mating wafers were bonded in clean ambient air. Only hand pressure was used to apply force after contacting at the center of the mating wafers. The bonding pressure was approximately 1–2 MPa. The wafers bonded in the atmospheric air were kept in the atmospheric air for 24 h to saturate the bonding strength.

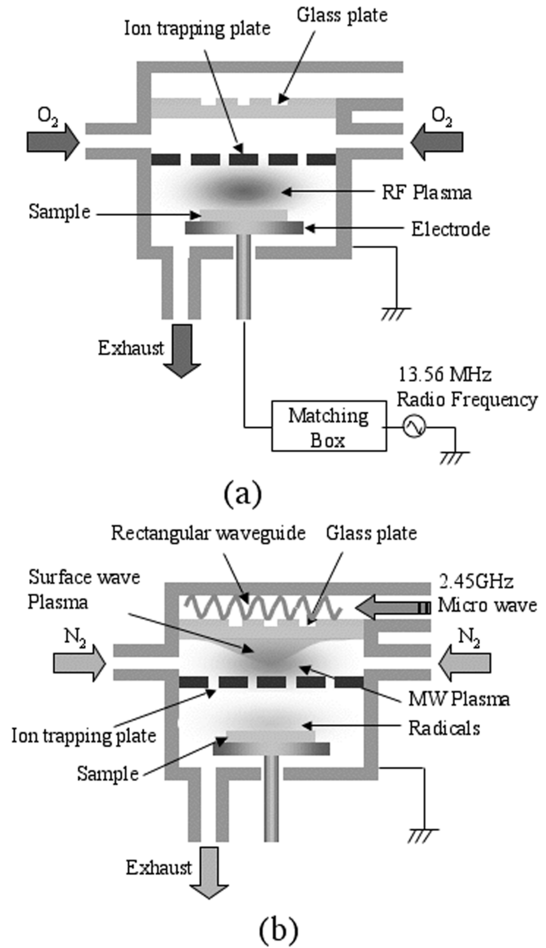

Fig. 1. Schematic diagrams for (a) RF O_2 RIE plasma system with self-biased condition and (b) modified N_2 radical MW plasma system. The plasma was generated one after another to activate the wafer surfaces.

TABLE I
GENERATING CONDITIONS FOR O_2 RIE AND N_2 RADICAL PLASMA WITH PROCESSING TIME FOR THE ACTIVATION OF SI AND GLASS WAFERS

Plasma type	O_2	N_2
Discharge mode	RIE	Radical
Chamber pressure (Pa)	30	100
Discharge power (W)	200	2000
Process time (s)	60	60

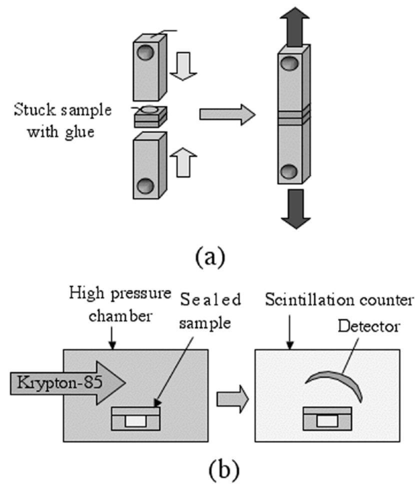

Fig. 2. Schematic diagrams for (a) tensile pulling test for the evaluation of strength of bonded wafers and (b) fine leak test for the evaluation of sealing behavior of cavities.

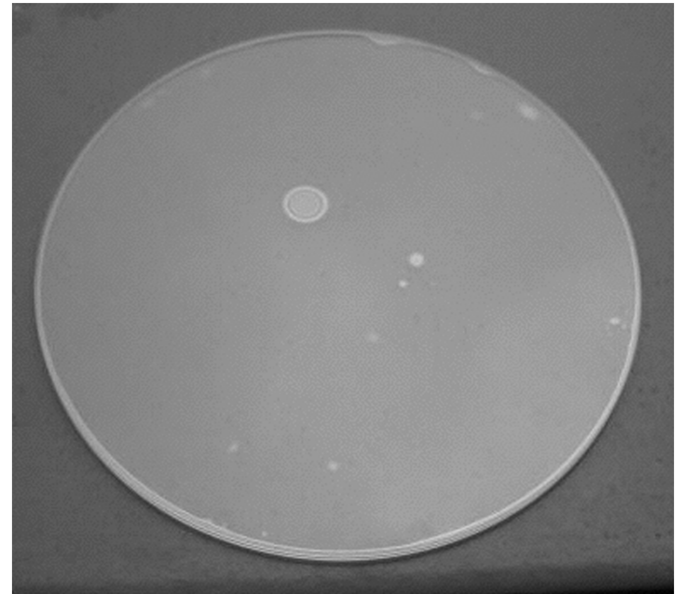

Fig. 3. Wafer-level optical image of 5-in bare glass/glass wafers bonded in the atmospheric air using the sequential plasma activation process at room temperature.

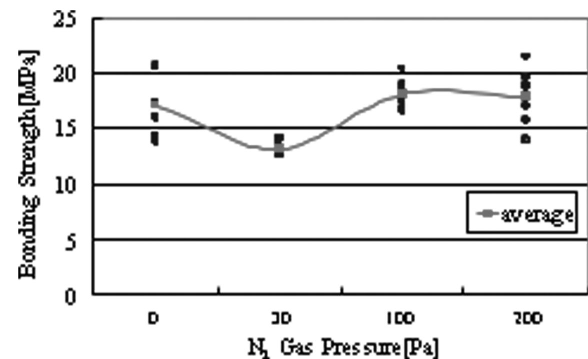

Fig. 4. Dependence of N_2 gas pressure on the bonding strength of bare glass/bare glass wafers. The wafers were activated with O_2 RIE at 30 Pa for 60 s prior to N_2 radical treatment for 60 s at various N_2 pressure.

B. Tensile Pulling and Leak Tests

Bond strength was measured by a tensile pulling tester (AGS-1 kNG), which was made by the Shimadzu Corporation. The bonded wafers were cut into 10×10 mm^2 pieces and stuck to metal bars (jigs) with glue for the tensile pulling test. Fig. 2(a) and (b) shows the schematics for the tensile pulling and fine leak tests, respectively. For fine leak test, the sealed cavities of Si/glass and glass/glass (will appear in the results and discussion section) were placed in a high pressure of radioisotope Kr-85 gas mixture chamber and then measured the radiation counts coming out from the sealed cavities by scintillation counter outside the chamber as shown in Fig. 2(b).

III. Results and Discussion

A. Glass/Glass Bonding

Fig. 3 shows the optical image of 4-in glass/glass wafers bonded by using the sequential plasma activation process at room temperature. The wafers surfaces were activated with O_2 RIE and N_2 radical at 30 Pa for 60 s. The entire area was bonded except a few small voids. The unbonded region can be due to failure of removing particles from the mating surfaces after plasma cleaning. The bonding experiments were performed in the atmospheric air of a class 10 000 clean room. Therefore, the dust/particles problem could be minimized with handling of wafers during bonding in a better clean room environment.

Fig. 4 shows the influence of N_2 pressure on the bonding strength of bare glass/bare glass wafers bonded at room temperature in the atmospheric air. At 30-Pa N_2 pressure, the data scattering was minimum, whereas it was maximum at 200 Pa. In addition, the tensile pulling results shown includes the bonding strength for the samples which were debonded not only from the bulk of glass wafers, but also from the glue used for placing the samples surfaces on the tensile jigs and from the interface of the samples. So, the prediction of the exact reasons responsible for the slight increase of the tensile strength after 30-Pa N_2 pressure was difficult. The difficulty of measuring tensile strength of bare wafers bonded is well known [13]. Mesa structured bonded wafers are known to reduce artifacts on the bonding strength measured by the tensile pulling test. Therefore, mesa structures were prepared on the surface of one wafer of mating pairs for the quantitative measurement of the tensile bond strength as shown in Fig. 5. The optical image for bare/mesa structured glass wafers was identical to that of the bare/bare glass wafers. The height and width of the mesa structures were 4 μm and 2 mm, respectively. During dicing, not a single chip was debonded.

Fig. 6 shows the nitrogen gas pressure dependence on the bonding strength of the mesa structured glass/bare glass wafers bonded by using the sequential plasma activation process at room temperature. This figure also includes the surface roughness of glass wafers measured by an atomic force microscope (AFM) (Seiko Instruments), which were prepared under identical conditions of the bonding experiments as a function N_2 gas pressure. The scanning area was (1×1) μm^2. Bond strength and surface roughness were expressed by the curves and the column bars, respectively. All of the samples were visually debonded from the interface after tensile pulling tests, indicating that the

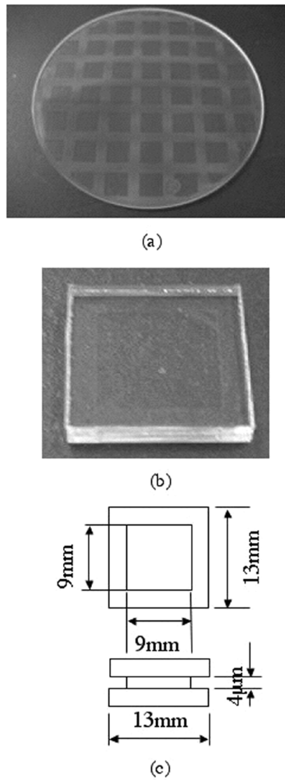

Fig. 5. (a) Wafer-level optical image of bare and patterned glass wafers. (b) Chip-size optical image of bare and patterned glass wafers after dicing. (c) Schematic diagrams for the dimensions of a single chip. The mesa height was 4 μm.

intrinsic interface strength of the glass/glass wafers is weak. The standard deviations of the tensile strength were exceedingly high and which were 86.5, 50.9, 99.9, and 68.1% deviated from the mean values at the N_2 radical pressure of 0, 30, 100, and 200 Pa, respectively. At 0 and 100 Pa pressures, the deviations were near to 100%. At 30 and 200 Pa, the deviations were almost identical. The mean tensile strength values can be seen in Table II. Considering that the bonding strength with the increase of N_2 pressure appeared to the upper deviation level, it could be roughly concluded that the bonding strength increased with the increase of N_2 radical pressure. The bonding strength might vary with different inclusions, such as dust/particles at the interface, inhomogeneous force application to the surfaces due to parallelism problem of the jigs and their angles during pulling test, inhomogeneous plasma etching of the surfaces, etc., resulting in broader scatter in bond strength. The intensity of O_2 RIE and N_2 radical plasma was almost homogeneous. However, the surface roughness, as shown in Table II, can be another parameter to control the bonding strength. Before plasma activation, the root mean square (rms) surface roughness of the glass wafers was 0.3 nm, and it was 0.9 nm after activation with O_2 RIE plasma (which is the value at 0 (no N_2 radicals) Pa of N_2 pressure) for 60 s at 30 Pa. The rms surface roughness increased with the increase of N_2 gas pressure, which is consistent to the results of other work [14]. The rms value for 30 Pa N_2 pressure was 1 nm. At 200 Pa, it was almost three times higher than that of 30-Pa pressure (Table II). Therefore, strong influence of N_2 pressure was observed, and the optimum pressure to increase the tensile strength was found to be 30 Pa.

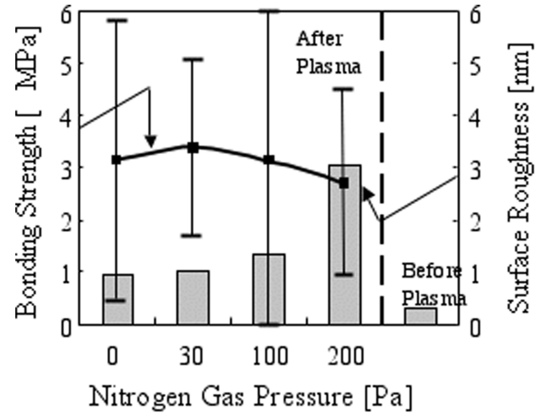

Fig. 6. Tensile strength of patterned glass/bare glass wafers as a function of N_2 gas pressure.

TABLE II
SURFACE ROUGHNESS OF GLASS WAFERS ALONG WITH MEAN TENSILE STRENGTH AND STANDARD DEVIATION AT VARIOUS N_2 GAS PRESSURE. "WITHOUT PLASMA" INDICATES THE SURFACE ROUGHNESS OF VIRGIN GLASS WAFER. THE SCANNING AREA WAS $(1 \times 1)\ \mu m^2$

N_2 Pressure (Pa)	Surface roughness (rms)	Standard deviation (%)	Mean tensile strength (MPa)
0	0.9	86.5	3.2±1.1
30	1.0	50.9	3.5±0.6
100	1.4	99.9	3.2±1.2
200	3.1	68.1	2.7±0.8
Without plasma	0.3	–	–

A significant difference in the absolute tensile strength between the bare/bare (Fig. 4) and bare/patterned (Fig. 6) glass wafers was found. Nevertheless, the bonding experiments were performed at the identical conditions. Probably, discrepant fracture mechanics and surface states are responsible for this difference. When a tensile tester pulls from opposite directions perpendicularly to the bonded surfaces to separate surfaces, the stress on the bonded surfaces surrounding the jigs can be compressive for the bare/bare bonded wafers. On the other hand, it can be a combination of compressive and tensile for the bare/mesa wafers. Long chemical etching and sequential plasma processes of mesa wafers might have generated porous surfaces including pinholes, which can work as tensile force and easily allow air across the interface during tensile pulling test. As mentioned previously, only hand pressure was used to apply force after contacting the mating wafers in the atmospheric air to propagate the bonding area. Faster propagation of bonding in the bare/mesa structured wafers than that of the bare/bare wafers was observed. The faster propagation of bonding is probably because the surface layer of air has a shorter distance to go in the mesa wafer than in the bare wafer. This also can be due to the plasma-induced polar dangling bonds on the surfaces [15] and their relationship with the surface structure. Further investigation is necessary to gain insights into the detailed mechanism.

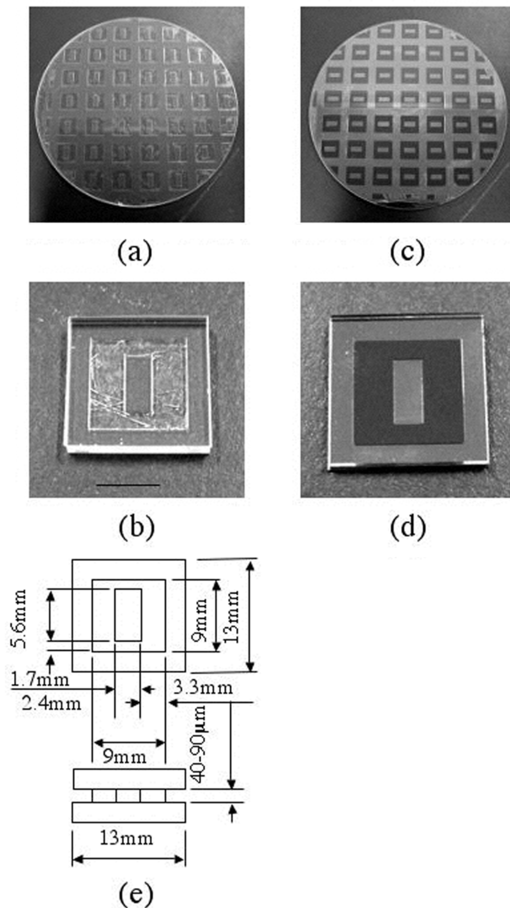

Fig. 7. Typical optical images of (a) glass/glass cavities on 4-in wafers. (b) Single glass/glass chip with a cavity after dicing. (c) Si/glass cavities on 4-in wafers. (d) Single Si/glass chip with a cavity. (e) Dimensions of a single chip with a cavity. The sealed cavities were used for fine leak test. All chips were survived after dicing.

B. Sealing Behavior of Si/Glass and Glass/Glass

To investigate the sealing behavior of Si/glass and glass/glass bonded by the sequential plasma activation process, cavities of sizes $5.6 \times 2.4 \times$"0.04–0.09" mm^3 were fabricated on Si and glass wafers. Si and glass wafers were etched with tetra-methyl ammonium hydroxide (TMAH) and BHF, respectively. The bottom of the glass wafer was coated also with photo resist to withstand long etching with BHF required for deep cavities. Fig. 7(a) and (c) shows the optical images of wafer-level Si/glass and glass/glass interfaces, respectively. The bonded wafers were cut into chips of sizes of 13×13 mm^2 for the radioisotope fine leak test. Not a single chip was debonded during dicing, and the typical optical images for diced chips are shown in Fig. 7(b) and (d). Fig. 7(d) shows the dimensions of a single chip with the mesa structures and the cavity. The horizontal and vertical sealed widths of the cavity were 3.3 and 1.7 mm. The whole chip area with the cavity was 9×9 mm^2. A remarkable difference in the optical images of a single chip of glass/glass [Fig. 7(b)] and Si/glass [Fig. 7(d)] interfaces was found. The dirty optical image for the glass/glass interface surrounding the cavity was due to the influence of chemical etching and photo lithography on photo resist of the bottom surface.

Sealed cavities of Si/glass and glass/glass wafers were exposed to a mixture of Kripton-85 gas of specific radioactivity of

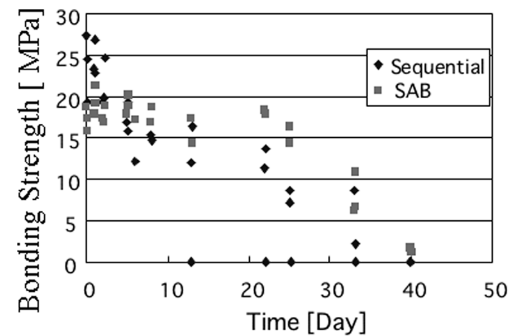

Fig. 8. Bonding strength of Si/Si as a function of dipping time in the 3% hydrofluoric acid at room temperature.

1.6×10^{12} Bq/m^3 in a background high pressure of 5×10^5 Pa for 15 h in order to measure the leak rate of the cavities [Fig. 2(b)]. Total numbers of cavities used for the fine leak tests were eight for each category. The background dose was 71–95 counts per min (cpm). The leak rate of exposed cavities was measured outside the chamber by measuring radiation counts coming out of the sealed cavities using a scintillation counter. The estimated leak rate was lower than 1.0×10^{-9} Pa m^3/s. Since the cavity volume was about 1.0×10^{-9} m^3, the leak rate for the Si/glass and glass/glass cavities satisfies to the requirements of 1.0×10^{-9} Pa m^3/s for MIL-STD-883E [16] encapsulation standard in hazard environments.

Fig. 8 shows the time-dependent influence of the HF acid on the bonding strength of Si/Si interface prepared by the SAB and the sequential plasma activation processes at room temperature. The main reason for using HF is to see whether the interfaces can withstand a highly reactive chemical. In the SAB process, 8-in Si wafers were activated with an Ar-low energy ion source of 80 V and 3 A for 10 s and bonded in a vacuum pressure of 10^{-7} Pa. Sequentially treated samples were activated with O_2 RIE and N_2 radical for 60 s. Chip size samples cut from the 8-in Si/Si wafers were dipped in the 3% HF for 40 days. In the SAB processed interfaces, the bonding strength remained constant for 20 days and then decreased in the increase of dipping time. On the other hand, in the case of the sequentially processed interfaces, the bonding strength decreased in the increase of dipping time from the beginning of the experiments. Faster decrease in the tensile strength of sequentially processed Si/Si interface was due to the etching of oxides across the interface, whose thickness was much larger than that of the SAB processed Si/Si interface. The comparative chemical reliability of the Si/Si interfaces processed by the low energy activation and plasma activation after dipping in water, ethanol, acetone, and 3% HF for 30 days at room temperature showed the substantial dependence of tensile strength on the chemical types. The bonding strength was not noticeably degraded in any chemical except in HF. The remarkable difference in the tensile strength of the SAB and plasma-processed interfaces dipped in HF was likely be controlled by the discrepant surface chemical reactions at the interfaces.

C. Role of N_2 Radical and Bonding Mechanism

To clarify the role of N_2 radical on the sequential plasma activation bonding process and the bonding mechanism, chemical information of glass wafers before and after surface activation

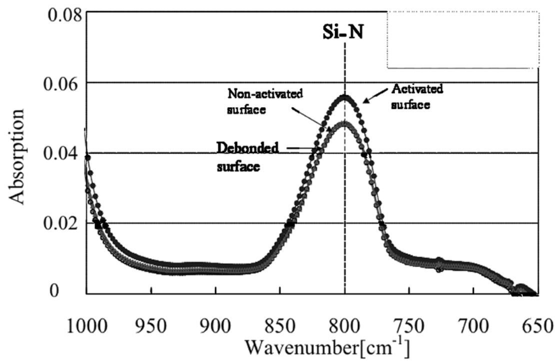

Fig. 9. FTIR spectra for activated, nonactivated, and debonded glass wafer surfaces. The wafer surfaces were activated with O_2 RIE plasma and N_2 radical plasma at 30 Pa for 60 s.

with plasma and after debonding were systematically investigated by using Fourier transform infrared spectroscopy (FTIR) measurements. Fig. 9 shows the comparison of the FTIR spectra for glass before plasma, after plasma, and after debonding. The activation time and gas pressure for O_2 RIE and N_2 radical were 60 s and 30 Pa, respectively. The spectra show an intense peak for the sequentially plasma treated sample at the wavenumber of 800 cm^{-1}. N_2 radical, which chemically activates the surface, can bind with Si and O_2 and partly implant in the glass. Therefore, N_2 radical possibly contribute to the silicon oxinitride. Silicon oxinitride absorption behavior has been reported be varied near 850 cm^{-1} depending on the nitrogen-to-oxygen ratio [17]. Identical motivation drove us to investigate the microstructure of the bonded interface of Si wafers, which were activated with O_2 RIE plasma for 60 s and N_2 radical for 10 and 1200 s [18]. Radiation-induced amorphous layer at the Si/Si interface was found, which was indicative of distorted short range order of Si atoms. A new phase in both sides of Si across the amorphous layer was found probably due to the long exposure of Si surfaces with the N_2 MW radical. This new phase was detected at the Si/Si interface prepared after activating with O_2 RIE plasma for 60 s and N_2 radical for 10 s. Earlier investigation of the sequentially plasma treated (O_2 RIE for 60 s and N_2 radical for 60 s) Si surfaces by X-ray photoelectron spectroscopy (XPS) detected a few nitride nanolayers on the surface. The bonding energy for N 1-s peak was higher than that of silicon oxinitride, which was believed be due to the meta-stable N–O bonding [19]. Silicon nitridation has also been reported by utilizing an RF N_2 radical irradiation SiO_2 [20], [21]. Therefore, the strong bonding results could be interpreted in terms of the reaction between the plasma-induced metastable surfaces through OH sites on both surfaces (when the O_2 RIE and N_2 radically treated Si surface exposed to the atmospheric air for bonding), which resulted in water formation across the interface. As the water diffused with time into bulk materials, ON sites on both surfaces reacted and produced stabilized silicon oxinitride resulting in strong bonding strength. Long exposure of N_2 MW radical plasma might diffuse N_2 in the bulk of Si.

In order to gain insights into the bonding mechanism of the sequential plasma activation process, this process should be comparatively explained with other direct bonding processes for Si/Si and Si/SiO_2. Direct wafer bonding can be categorized into hydrophilic, plasma assisted hydrophilic, and hydrophobic bonding processes. High-temperature annealing is required after bonding to achieve high bonding strength in all of the processes, whereas no annealing is essential in the sequential plasma activation process. In general, Si and SiO_2 hydrophilic surfaces are obtained by RCA (NH_4OH:H_2O_2:H_2O = 1:1:5 and HCl:H_2O_2:H_2O = 1:1:6) cleaning technique in which the surfaces are covered with OH groups after cleaning. In hydrophilic plasma-assisted bonding, the hydrophilic surfaces are exposed to O_2 plasma, which results in OH-groups termination on native oxide layers (about a 1-nm thick) on the surfaces. Sometimes the plasma-exposed surfaces are dipped into water and the hydrophilic surfaces absorb water molecules on their silanol (Si-OH) groups. If the hydrophilic surfaces are either exposed to O_2 and/or dipped into water followed by contact, the two opposite surfaces are linked by weak hydrogen bonds of absorbed water molecules. The long hydrogen bridge between the mating surfaces can be shortened by the diffusion of water molecules into the silicon bulk during heating at elevated temperatures. High-temperature annealing forms strong covalent bonding of Si–O–Si. In the case of hydrophobic bonding, the wafer is dipped into a HF solution to remove the native oxides, and the surfaces are terminated mainly by hydrogen and partly by fluorine. The hydrogen-terminated silicon surfaces interact through van der Waals forces. Hydrogen atoms are released from the surface at the interface and diffused into silicon bulk during annealing at $\geq$ 300°C resulting in the formation of strong covalent bonding of Si–Si. A more detailed description of the hydrophilic and hydrophobic bonding mechanisms can be found in [22]. On the other hand, as previously mentioned, physical sputtering of O_2 RIE plasma was used to remove native oxides of Si or SiO_2 and to generate oxide layers on the nonchemically cleaned surfaces in the sequential plasma activation process. Subsequent activation (of the surfaces which were physically treated with O_2 RIE) with N_2 MW radical can produce thermodynamically and chemically metastable oxynitride layers. When the metastable oxynitride surfaces are exposed to atmospheric air with moderate humidity, water molecules are stuck on the surfaces. Thus, a set of chemical reactions both during the surface preparation (by the physical sputtering of O_2 RIE plasma combined with the chemical activation of N_2 MW plasma) and under mating the two metastable oxynitride surfaces are plausible mechanism responsible for the bonding of glass/glass in the sequential plasma activation process without any wet chemicals. Nevertheless, the reactions between the two metastable surfaces result in a stabilized silicon oxynitride network at the interface. Silicon oxynitride network is most likely distributed in the amorphous region as well.

D. Microfluidic Devices

Recently, microelectronics, MEMS, biological, and chemical sciences and technologies are being merged together. Gomez *et al.* [23] reported microfluidics biochip fabrication for the interrogation of biological species such as molecules, cells, etc. The total fluidic path volume was 30 nL. Based on the measurement of a low conductivity ionic strength of suspension medium modified by the bacterial metabolism, biological species can be

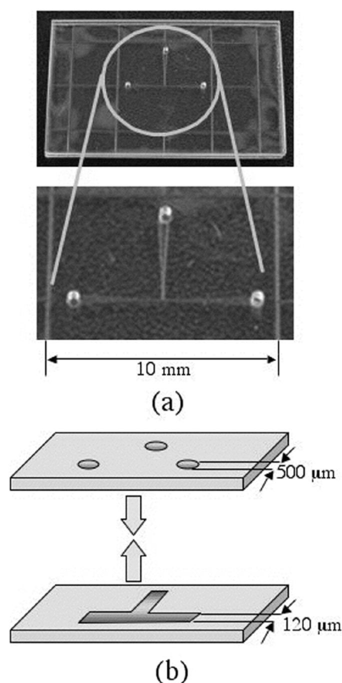

Fig. 10. (a) Optical images of microfluidics devices fabricated with glass wafers. (b) Dimensions for top and bottom glass wafers with holes and T-channels, respectively. Sequential plasma activation process was used to bond the two glass wafers having structures at room temperature.

detected. The main features of the microfluidic device were the fabrication of channels on Si, deposition of SiO_2, fabrication of metal electrodes for impedance measurements, and sealing using glass cover with spin-on-glass as intermediate layer. The bonded samples heated at 300 °C were cracked due to large thermal expansion (CTE) mismatch problem. Bonding succeeded when heating only to 200 °C, which could withstand up 340 kPa. When the microfluidic flow pressure increased to 700 kPa, the bonded interface was debonded. Therefore, low-temperature hermetic sealing of Si/glass and glass/glass is an important criterion for the microfluidic application.

Fig. 10 shows the optical images of glass/glass bonding for microfluidic applications. Chip size glass wafers were used. One glass wafer had 500 μm size three holes, which were made by using mechanical mounting wheels drilling process. The other glass chip had T-shape microfluidic channels fabricated by the wet chemical (HF) etching process. The depth and width of the microchannels was 60 and 120 μm, respectively. The chip size drilled wafers were polished by mechanical and chemical polishing to smooth the surfaces, then activated with sequential plasma activation process, and finally bonded together after manual aligning at room temperature. The bonding strength was equivalent to the bulk materials. In other words, no interface fracture was evident after the tensile pulling tests. Glass is transparent to the ultraviolet (UV) light at wavelengths greater than 350 nm. On the other hand, the Ar-low-energy ion beam with 80 eV and 3 A showed no significant influences on the UV transmittance properties of quartz wafers irradiated for 30 min [12]. Therefore, laser induced fluorescence [24] and UV absorbance detections [25] of microfluidics are possible when flowing through the glass/glass microfluidics devices. Identical microfluidics biochip fabrication, which was reported in the [23], can be realized with the help of the sequential plasma activation process. Wafer-level packaging of microfluidics channels on Si and glass wafers appears to be feasible contingent upon the controlled warpage/waviness of wafers. For wafer-level packaging, the minimum coplanarity of 4- and 8-in Si and glass wafers should be controlled to 3 and 6 μm, respectively.

Furthermore, living cells can be preserved in the glass/glass microfluidics sealed/closed cavities for detection because of the room-temperature bonding of glass/glass in the atmospheric air after sequential plasma activation [26]. Based on the high bonding strength and hermetic sealing behavior Si/glass and glass/glass wafers with structures and microchannels bonded by the sequential plasma activation including the preserving feasibility of living cells in the microchips, it can be used for the microfluidics packaging.

IV. Conclusion

Glass/glass wafers were integrated for the first time in the atmospheric air at room temperature by new sequential plasma activation bonding process, in which surfaces were cleaned with O_2 radio frequency (RF) reactive ion etching (RIE) plasma followed by N_2 microwave radicals. The bonded interface was very strong and the bond strength was comparable to bulk materials. Bond strength considerably increased with the nitrogen radical treatment after oxygen RIE activation prior to bonding. Chemical reliability tests showed that the bonded interfaces were significantly robust when exposed to various chemicals. Si/glass and glass/glass cavities formed by the sequential plasma activation process showed a hermetic sealing behavior. SiO_xN_y was observed in the sequentially plasma-treated glass wafer, probably due to the binding of nitrogen with Si and oxygen and the implantation of N_2 radical in the wafer. High bonding strength was thought to be due to a diffusion of absorbing water into the wafer surface and a reaction between silicon oxynitride layers on the mating wafers. This process was successfully demonstrated by fabrication of T-shape microfluidics channels on glass wafers by bulk micromachining and sealing with a flat cover glass.

Acknowledgment

The authors would like to thank the Toso Company, Ltd., Japan, for supplying glass wafers as a part of collaborative work. They would also like to thank Dr. T. Nisisako of the University of Tokyo is for his assistance in the fabrication of the microfluidic channels. They would also like to thank Prof. M. J. Kim of the University of Texas at Dallas for his critical review and comments of the article.

References

[1] J. Khandurina, T. E. McKnight, S. C. Jacobson, L. C. Waters, R. S. Foote, and J. M. Ramsey, "Integrated system for rapid PCR-based DNA analysis in microfluidic devices," *Anal. Chem.*, vol. 72, pp. 2995–3000, 2000.

[2] Y. Liu, D. Ganser, A. Schneider, R. Liu, P. Grodzinski, and N. Kroutchinina, "Microfabricated polycarbonate CE devices for DNA analysis," *Anal. Chem.*, vol. 73, pp. 4196–4201, 2001.

[3] T. McCreedy, "Fabrication techniques and materials commonly used for the production of microreactors and micro total analytical systems," *Trends Anal. Chem.*, vol. 19, no. 6, pp. 396–401, 2000.

[4] A. Berthold, L. Nicola, P. M. Sarro, and M. J. Vellekoop, "Glass-to glass anodic bonding with standard IC technology thin films as intermediate layers," *Sens. Actuators*, vol. 82, pp. 224–228, 2000.

[5] V. G. Kutchoukov, F. Laugere, W. van der Vlist, L. Pakula, Y. Garini, and A. Bossche, "Fabrication of nanofluidic devices using galss-to-Glass anodic bonding," *Sens. Actuators A*, vol. 114, pp. 521–527, 2004.

[6] D.-J. Lee, Y.-H. Lee, J. Jang, and B.-K. Ju, "Glass-to-Glass electrostatic bonding with intermediate amorphous silicon film for vacuum packaging of microelectronics and its application," *Sens. Actuators A*, vol. 89, pp. 43–48, 2001.

[7] S. Toumikoski and S. Franssila, "Free-standing SU-8 microfluidic chips by adhesive bonding and release etching," *Sens. Actuators A*, vol. 120, no. 2, pp. 408–415, 2005.

[8] D. J. Harrison, A. Manz, Z. Fan, H. Ludi, and H. M. Widmer, "Capillary electrophoresis and sample injection systems integrated on a planar glass chip," *Anal. Chem.*, vol. 64, pp. 1926–1932, 1992.

[9] S. C. Jacobson, R. Hergenroder, L. B. Koutny, R. J. Warmack, and J. M. Ramsey, "Effects of injection schemes and column geometry on the perfomance of microchip electrophoresis devices," *Anal. Chem.*, vol. 66, pp. 1107–1113, 1994.

[10] H. Takagi, R. Maeda, T. R. Chung, and T. Suga, "Low temperature direct bonding of silicon and silicon dioxide by the surface activation method," *Sens. Actuators A*, vol. 70, pp. 164–170, 1998.

[11] T. Suni, K. Henttinen, I. Suni, and J. Makinen, "Effects of plasma activation on hydrophilic bonding of Si and SiO_2," *J. Electrochem. Soc.*, vol. 149, no. 6, pp. G348–G351, 2002.

[12] M. M. R. Howlader, H. Okada, T. H. Kim, T. Itoh, and T. Suga, "Wafer-level surface-activated bonding tool for MEMS packaging," *J. Electrochem. Soc.*, vol. 151, no. 7, pp. G461–G467, 2004.

[13] M. M. Visser, S. Weichel, R. de Reus, and A. B. Hanneborg, "Strength and leak testing of plasma-activated bonded interface," *Sens. Actuators A*, vol. 97–98, pp. 434–440, 2002.

[14] H. Takagi, R. Maeda, T. R. Chung, N. Hosoda, and T. Suga, "Effect of surface roughness on room temperature wafer bonding by beam surface activation," *Jpn. J. Appl. Phys.*, vol. 37, pp. 4197–4203, 1998.

[15] M. Weigand, M. Reiche, and U. Gosele, "Time-Dependent surface properties and bonding of O_2-plasma-treated silicon (100) surfaces," *J. Electrochem. Soc.*, vol. 147, no. 7, pp. 2734–2740, 2000.

[16] *Test Method Standard, Micro-Circuits*, MIL-STD-883E, 1995.

[17] J. Lu, G. Rozgonyi, J. Rand, and R. Jonczyk, "Secondary phase inclusions in polycrystalline sheet silicon," *J. Crys. Growth*, vol. 269, pp. 599–605, 2004.

[18] H. Itoh, M. M. R. Howlader, H. Li, T. Suga, and M. J. Kim, "Combined process of radical and RIE for Si direct bonding," in *Proc Int. Conf. Electron. Packag. ICEP*, Tokyo, Japan, Apr. 13–15, 2005, pp. 94–99.

[19] T. Suga, T. H. Kim, and M. M. R. Howlader, "Combined process for wafer direct bonding by means of the surface activation method," in *Proc 54th Electron. Compon. Technol. Conf*, Las Vega, NV, Jun. 1–4, 2004, pp. 484–490.

[20] Y. Maeyama, H. Yano, Y. Furumoto, T. Hatayama, Y. Uraoka, and T. Fuyuki, "Improvement of SiO_2/SiC interface properties by nitrogen radical irradiation," *Jpn. J. Appl. Phys.*, vol. 42, pp. L575–L577, 2003.

[21] R. Takahashi, Y. Kobayashi, H. Ikeda, M. Sakashita, O. Nakatsuka, A. Sakai, S. Zaima, and A. Yasuda, "Scanning tunneling microscopy of intital nitridation processes on oxidized Si(100) surface with radical nitrogen," *Jpn. J. Appl. Phys.*, vol. 42, pp. 1966–1970, 2003.

[22] Q.-Y. Tong and U. Gosele, *Semiconductor Wafer Bonding: Science and Technology*. New York: Wiley, 1999.

[23] R. Gomez, R. Bashir, A. Sarikaya, M. R. Ladisch, J. Sturgis, J. P. Robinson, T. Geng, A. K. Bhunia, H. L. Apple, and S. Wereley, "Microfluidic biochip for impedance spectroscopy of biological species," *Biomed. Microdevices*, vol. 3:3, pp. 201–209, 2001.

[24] Z. Liang, N. Chiem, G. Ocvirk, T. Tang, K. Fluri, and D. J. Harrison, "Microfabrication of a planar absorbance and fluorescence cell for integarted capillary electrophoresis devices," *Anal. Chem.*, vol. 68, pp. 1040–1046, 1996.

[25] L. Ceriotti, K. Weible, N. F. de Rooij, and E. Verpoorte, "Rectangular channnels for lab-on-a-Chip applications," *Microelectron. Eng.*, vol. 67–68, pp. 865–871, 2003.

[26] G. R. Fuhr and C. Reichle, "Living cells in opto-electrical cages," *Trends Anal. Chem.*, vol. 19, no. 6, pp. 402–409, 2000.

M. M. R. Howlader received the B.Sc.Eng. degree in electrical and electronic engineering from Khulna University of Engineering and Technology, Khulna, Bangladesh, in 1988 and the M.S. and Ph.D. degrees in nuclear engineering from Kyushu University, Fukuoka, Japan, in 1996 and 1999, respectively.

He was awarded one year as a Postdoctoral Scholar at University of California at Davis in 1999 and worked on radiation effects on materials. From 2000 to 2005, he was with the Research Center for Advanced Science and Technology, University of Tokyo, Tokyo, Japan, as a member of faculty, where he was an endowed Associate Professor with the center. He is currently with the Engineering Physics Department and Electrical and Computer Engineering Department, McMaster University, Hamilton, ON, Canada. He holds two patents and has published 20 technical papers and over 50 international proceeding articles. His research focuses on the chip-size and wafer-level integration for microelectronics, microelectromechanical systems, and optoelectronics packaging, oxidation behavior of solders and electronic materials, interfacial adhesions, radiation effects on materials and packages.

Dr. Howlader is a member of Japan Institute of Electronic Packaging (JIEP) and he received the Best Technical Paper Award at the International Conference on Electronic Packaging in 2003.

S. Suehara received the B.S. the degree in mechanical engineering from Tokyo University of Agriculture and Technology, Tokyo, Japan, in 2003 and the M.S. degree in precision engineering from the University of Tokyo, Tokyo, in 2005.

Currently, he is with the Terumo Corporation, Ltd., Tokyo.

H. Takagi received the M.Sc.Eng. degree in precision engineering and the Ph.D. degree in engineering from the University of Tokyo, Tokyo, Japan, in 1991 and 1999, respectively.

In 1991, he joined the Mechanical Engineering Laboratory, Ministry of International Trade and Industry (MITI). He is currently a Senior Research Scientist in Advanced Manufacturing Reseach Institute (AMRI), National Institute of Advanced Industrial Science and Technology (AIST), Ibaraki, Japan. His research interests are wafer bonding technologies, especially low-temperature processes, and their applications for microelectromechanical systems (MEMS), information, telecommunication devices, and so on. He has published 10 journal papers and over 20 international conference papers.

Dr. Takagi is a member of Japan Institute of Electronic Packaging (JIEP), Japan Society of Precision Engineering (JSPE), Japan Society for Applied Physics (JSAP), and Japan Institute of Metals (JIM).

T. H. Kim received the Ph.D. degree in engineering from the University of Tokyo, Tokyo, Japan, in 2004.

Currently, he is with LG Electronics, Seoul, South Korea. His research interests include wafer bonding, microelectronic packaging, and optical packaging.

R. Maeda received the M.Sc. degree in engineering from the University of Tokyo, Tokyo, Japan, in 1980 and the Ph.D. degree in engineering from the Chiba Institute of Technology, Chiba, Japan, in 2001.

He joined Mechanical Engineering Laboratory, Ministry of International Trade and Industry (MITI), in 1980. He is now the Group Leader of Integrated Solid-state Electro Mechanical Instruments (ISEMI), National Institute of Advanced Industrial Science and Technology (AIST), Ibaraki, Japan. His research interests include three-dimensional microstructuring and forming, piezoelectric microactuators, and MEMS packaging. He has published more than 100 journal papers and 150 international conference proceedings.

Dr. Maeda is a member of the Japan Institute of Electronic Packaging (JIEP), the Japan Society of Precision Engineering (JSPE), the Institute of Electrical Engineers in Japan (IEEJ), and the Japan Institute of Metals (JIM).

T. Suga received the M.S. degree in precision engineering from the University of Tokyo, Tokyo, Japan, in 1979 and the Ph.D. degree in metallurgy and materials science from University of Stuttgart, Stuttgart, Germany, in 1983.

He joined the Max-Planck Institute for Metal Research, Stuttgart, in 1979, where he studied metal–ceramic joining and fracture mechanics of interfaces. In 1984, he became a member of the Faculty of Engineering, University of Tokyo, as an Associate Professor. Since 1993, he has been a Professor of precision engineering, working in the field of materials interfaces and microsystem integration. He is also conducting a research group in the National Institute of Materials Science (NIMS), Tsukuba. His researches focus on microelectronics and microsystems packaging, as well as development of key technology, especially bonding technology. Especially, the feasibility of the room-temperature bonding has been demonstrated by a series of his studies over the past ten years. He has endeavored to establish collaboration between industries and academic societies for the packaging technology. He organized the foundation of the Institute of Micro-System Integration (IMSI) in 1997, which is the first consortium for the competitive packaging industry, consisting currently of 30 Japanese companies. He has also advocated the importance of environmental aspects of packaging technology and is well known as the key organizer of Japanese roadmap for lead-free soldering and eco-design conference. He has published 200 papers and five books in the field of material science and electronic packaging.

Dr. Suga is a member of board of directors of the Japan Institute of Electronic Packaging (JIEP) and Japan Insitute of Precision Engineeiring (JIPE).